

HIGHLIGHTS AND BREAKTHROUGHS

News and views on elastic geobarometry: Mazzucchelli et al. (2020)

Fabrizio Nestola

Dipartimento di Geoscienze, Università degli Studi di Padova, Via G. Gradenigo, 6, I-35131 Padova, Italy

E-mail: fabrizio.nestola@unipd.it

Pressure and temperature estimates of rocks provide the fundamental data for the investigation of many geological processes such as subduction and exhumation and yet there determination remains extremely challenging (Tajcmanova et al. 2020). A wide variety of methods are constantly being developed to tackle the ambitious objective of pinpointing the geological history of rocks through the many complex processes often interacting to one another at depth in our planet. Analytical advances are being pushed to the limit of conventional methods, allowing information preserved by mineral, fluid and solid inclusions to be used for high spatial resolution determinations that can be used to unravel a large variety of processes occurring at the micro to nano scale. Among these, chemical geothermobarometry that is often challenging in many rock types due to alteration processes, chemical re-equilibration, diffusion, and kinetic limitations has been increasingly coupled with elastic geothermobarometry (e.g. Anzolini et al. 2019; Gonzalez et al. 2019). Elastic geothermobarometry on host-inclusion systems (see Figure 1 for an example) is a new and complementary non-destructive method to determine the pressures (P) and temperatures (T) of inclusion entrapment (i.e., the P-T conditions attained by rocks and minerals at depth in the Earth) from the remnant stress or strain measured in inclusions still trapped in their host mineral at room conditions (e.g. Nestola et al. 2011, Howell et al. 2012, Alvaro et al. 2020).

29 This method underwent significant developments in the past decade aimed overcoming
30 several serious restrictions to previously available models and methodologies, which have led to
31 questions being raised about the general validity of the method. Most of the recent developments
32 have been focused on enhancing the method to allow its application to a broader variety of
33 scenarios, overcoming the three major assumptions (i) linear elasticity (Angel et al. 2014); (ii)
34 spherical shape (Campomenosi et al. 2018; Mazzucchelli et al. 2018); (iii) isotropic elastic
35 properties for the host and the inclusion to allow its applications to an increasing number of host
36 inclusion pairs with a variety of analytical techniques (e.g. micro-Raman spectroscopy, Murri et
37 al. 2018) and calculation methods (e.g. non-linear elasticity and numerical modeling, Anzolini et
38 al. 2019; Mazzucchelli et al. 2019; Morganti et al. 2020).

39 This first part of the development essentially concerned the calculation of the mutual
40 elastic relaxation of the host and inclusion, for which initial estimates have relied on the
41 assumption of linear elasticity theory. Angel et al. (2014) presented a new formulation of the
42 problem that avoids this assumption and incorporates full non-linear elastic behavior for the host
43 and the inclusion and has been enhanced with the progressive implementation of carefully
44 validated equations of state for several host and inclusion phases (e.g. Angel et al. 2017a; Angel
45 et al. 2020; Mihailova et al. 2019; Milani et al. 2015; Milani et al. 2017; Murri et al. 2019;
46 Zaffiro et al. 2019). This finally allowed analyses incorporating the accurate behavior of quartz
47 inclusions in garnet over a large P and T interval (Angel et al. 2017a; Morana et al. 2020). The
48 methods and the calculation algorithm have been included in the freely available EoSFit-Pinc
49 software (Angel et al. 2017b). The availability of the new software and algorithm strongly
50 promoted the use of this methodology, enabling several researchers to perform their
51 measurements and calculations independently (Anzolini et al. 2019; Anzolini et al. 2018; Nestola
52 et al. 2016; Nestola et al. 2018a and 2018b; Nimis et al. 2016; Nimis et al. 2019).

53 The second part of development has been focused on measurements and calculations of
54 non-spherical inclusions in complex geometrical relationships with the host and/or other
55 inclusions. Such issues have been addressed with several numerical models on a variety of
56 shapes by Mazzucchelli et al. (2018), producing numerical correction factors to guide the readers
57 toward estimating the uncertainties associated with shapes different from spheres, including the
58 complex interplay of edges and corners for which only numerical solutions can be provided. In

59 Mazzucchelli et al. (2018), the authors estimated of the maximum discrepancies caused by
60 geometry and shape and validated their estimations against simple experimental results obtained
61 on mechanically polished, host inclusion systems by Campomenosi et al. (2018).

62 The most complex portion of development dealt with elastic the anisotropy of inclusions
63 as this is also the largest source of uncertainties that cannot be evaluated a priori simply looking
64 at the sample under the optical microscope, or with more complex techniques (e.g. Scanning
65 Electron Microscopy, X-ray micro-Tomography, *inter alia*). The importance of elastic
66 anisotropy essentially arises from the fact that an inclusion trapped in a host of any symmetry
67 exhumed to the lower P and T conditions at the Earth surface is subject to the strain imposed by
68 the host. The simplest, and yet still extremely complex, case that can be envisaged is that of a
69 cubic host (e.g. diamond) that we will consider nearly isotropic. In this case, after exhumation
70 the inclusion is subject to isotropic strains imposed by the host. An anisotropic inclusion subject
71 to isotropic strains must develop non-hydrostatic stresses (Angel et al. 2019; Murri et al. 2019;
72 Murri et al. 2018). This observation is sufficient to demonstrate that whatever tentative
73 interpretation of the measured state of stress for a non-isotropic inclusion in a isometric host
74 using conventional equations of state (as currently determined under hydrostatic compression) is
75 meaningless. However, several tentative steps have been made to try to estimate the effect of the
76 elastic anisotropy on (i) the calculation of the residual strain, stress and pressures; and (ii) the
77 calculation the entrapment conditions. For the calculation of the residual pressure, the major
78 issue arises from measurements performed via micro-Raman where most of the studies interpret
79 the peak shift of Raman bands ($\Delta\omega$) as a pressure effect using an empirical calibration that
80 relates Raman shift with P (e.g. Morana et al. 2020, Schmidt and Ziemann 2000). As already
81 shown by Grüneisen (1926) and later confirmed by Angel et al. (2019), and Murri et al. (2018
82 and 2019), this is physically incorrect as the Raman band shift depends upon the applied strains
83 through the Grüneisen tensor rather than the applied stress through a $\Delta\omega$ vs P calibration. This
84 fact may appear to have small effects when dealing with cubic hosts, but as shown by Bonazzi et
85 al. (2019) the effects become non-negligible at few GPa of entrapment. There are several
86 examples (Bonazzi et al. 2019; Gonzalez et al. 2019; Thomas and Spear 2018) of inclusions with
87 0 kbar of residual pressure calculated from the shift of the 464 cm^{-1} band that instead were
88 apparently entrapped at several kilobars, if calculations are performed via the Grüneisen tensor
89 approximation. These calculations from the Raman shift of multiple bands are now possible

90 through the software “Strainman” (Angel et al. 2019). The second part of the elastic anisotropy
91 contribution plays a crucial role in calculating the entrapment conditions starting from the strains
92 determined either from the Raman shifts or from the lattice parameters measured via X-ray
93 diffraction (e.g. Alvaro et al. 2020). This part has been addressed by the recent publication of
94 numerical and analytical solutions for non-isotropic, host-inclusion pairs presented in
95 Mazzucchelli et al. (2019) and Morganti et al. (2020).

96 The new EntraPT web application, published by Mazzucchelli et al. (2020) in *American*
97 *Mineralogist*, provides a platform for elastic geobarometry that includes these recent advances.
98 Thanks to this application, the user can interpret the residual strain of anisotropic inclusions in an
99 intuitive and consistent manner. Moreover, EntraPT, that is built on the underlying code of
100 Eosfit7c, provides the tools to perform calculations of the residual pressure and of the
101 entrapment pressure and temperature of isotropic and anisotropic systems using a self-consistent
102 set of thermoelastic properties (e.g. Alvaro et al. 2020; Gonzalez et al. 2019).

103

104 **References**

- 105 Alvaro, M., Mazzucchelli, M.L., Angel, R.J., Murri, M., Campomenosi, N., Scambelluri, M.,
106 Nestola, F., Korsakov, A., Tomilenko, A.A., Marone, F., and Morana, M. (2020) Fossil
107 subduction recorded by quartz from the coesite stability field. *Geology*, 48, 24-28.
- 108 Angel, R.J., Alvaro, M., and Nestola, F. (2017a) 40 years of mineral elasticity: a critical review
109 and a new parameterisation of equations of state for mantle olivines and diamond
110 inclusions. *Physics and Chemistry of Minerals*, 45), 95-113.
- 111 Angel, R.J., Alvaro, M., Schmid-Beurmann, P., and Kroll, H. (2020) Commentary on
112 “Constraints on the Equations of State of stiff anisotropic minerals: rutile, and the
113 implications for rutile elastic barometry” [*Mineralogical Magazine*, 83 (2019) pp. 339–
114 347]. *Mineralogical Magazine*, 84, 355-357.
- 115 Angel, R.J., Mazzucchelli, M.L., Alvaro, M., and Nestola, F. (2017b) EosFit-Pinc: A simple GUI
116 for host-inclusion elastic thermobarometry. *American Mineralogist*, 102, 1957-1960.
- 117 Angel, R.J., Mazzucchelli, M.L., Alvaro, M., Nimis, P., and Nestola, F. (2014) Geobarometry
118 from host-inclusion systems: the role of elastic relaxation. *American Mineralogist*, 99,
119 2146-2149.
- 120 Angel, R.J., Murri, M., Mihailova, B., and Alvaro, M. (2019) Stress, strain and Raman shifts.
121 *Zeitschrift fur kristallograhie - Crystalline Material*, 234, 129-140.
- 122 Anzolini, C., Nestola, F., Mazzucchelli, M.L., Alvaro, M., Nimis, P., Gianese, A., Morganti, S.,
123 Marone, F., Campione, M., Hutchison, M.T., and Harris, J.W. (2019) Depth of diamond
124 formation obtained from single periclase inclusions. *Geology*, 47, 219-222.

- 125 Anzolini, C., Prencipe, M., Alvaro, M., Romano, C., Vona, A., Lorenzon, S., Smith, E.M.,
126 Brenker, F.E., and Nestola, F. (2018) Depth of formation of super-deep diamonds:
127 Raman barometry of CaSiO₃-walstromite inclusions. *American Mineralogist*, 103, 69-74.
- 128 Bonazzi, M., Tumiati, S., Thomas, J.B., Angel, R.J., and Alvaro, M. (2019) Assessment of the
129 reliability of elastic geobarometry with quartz inclusions. *Lithos*, 350-351, Article n.
130 105201.
- 131 Campomenosi, N., Mazzucchelli, M.L., Mihailova, B.D., Scambelluri, M., Angel, R.J., Nestola,
132 F., Reali, A., and Alvaro, M. (2018) How geometry and anisotropy affect residual strain
133 in host inclusion system: coupling experimental and numerical approaches. *American*
134 *Mineralogist*, 103, 2032-2035.
- 135 Gonzalez, J.P., Thomas, J.B., Baldwin, S.L., and Alvaro, M. (2019) Quartz-in-garnet and Ti-in-
136 quartz thermobarometry: Methodology and first application to a quartzofeldspathic gneiss
137 from eastern Papua New Guinea. *Journal of Metamorphic Geology*, 37, 1193-1208.
- 138 Grüneisen, E. (1926) Zustand des festen Körpers. In C. Drucker, E. Grüneisen, P. Kohnstamm,
139 F. Körber, K. Scheel, E. Schrödinger, F. Simon, J.D. van der Waals, and F. Henning, Eds.
140 *Thermische Eigenschaften der Stoffe*, p. 1-59. Springer Berlin Heidelberg, Berlin,
141 Heidelberg.
- 142 Howell, D., Wood, I.G., Nestola, F., Nimis, P., Nasdala, L. (2012) Inclusions under remnant
143 pressure in diamond: a multi-technique approach. *European Journal of Mineralogy*, 24,
144 563-573.
- 145 Mazzucchelli, M.L., Angel, R.J., and Alvaro, M. (2020) EntraPT: an online platform for elastic
146 geothermobarometry. *American Mineralogist*,
- 147 Mazzucchelli, M.L., Burnley, P., Angel, R.J., Morganti, S., Domeneghetti, M.C., Nestola, F., and
148 Alvaro, M. (2018) Elastic geothermobarometry: corrections for the geometry of the host-
149 inclusion system. *Geology*, 46, 231-234.
- 150 Mazzucchelli, M.L., Reali, A., Morganti, S., Angel, R.J., and Alvaro, M. (2019) Elastic
151 geobarometry for anisotropic inclusions in cubic hosts. *Lithos*, 350-351, Article n.
152 105218.
- 153 Mihailova, B., Waesermann, N., Stangarone, C., Angel, R.J., Prencipe, M., and Alvaro, M.
154 (2019) The pressure-induced phase transition(s) of ZrSiO₄. *Physics and Chemistry of*
155 *Minerals*, 46, 807-814.
- 156 Milani, S., Angel, R.J., Scandolo, L., Mazzucchelli, M.L., Ballaran, T.B., Klemme, S.,
157 Domeneghetti, M.C., Miletich, R., Scheidl, K.S., Derzsi, M., Tokar, K., Prencipe, M.,
158 Alvaro, M., and Nestola, F. (2017) Thermo-elastic behavior of grossular garnet at high
159 pressures and temperatures. *American Mineralogist*, 102, 851-859.
- 160 Milani, S., Nestola, F., Alvaro, M., Pasqual, D., Mazzucchelli, M.L., Domeneghetti, M.C., and
161 Geiger, C.A. (2015) Diamond-garnet geobarometry: The role of garnet compressibility
162 and expansivity. *Lithos*, 227, 140-147.
- 163 Morana, M., Mihailova, B., Angel, R.J., and Alvaro, M. (2020) Quartz metastability at high
164 pressure: what new can we learn from polarized Raman spectroscopy? *Physics and*
165 *Chemistry of Minerals*, 47, doi: 10.1007/s00269-020-01100-y.
- 166 Morganti, S., Mazzucchelli, M.L., Alvaro, M., and Reali, A. (2020) A numerical application of
167 the Eshelby theory for geobarometry of non-ideal host-inclusion systems. *Meccanica*, 55,
168 751-764.

- 169 Murri, M., Alvaro, M., Angel, R.J., Prencipe, M., and Mihailova, B.D. (2019) The effects of
170 non-hydrostatic stress on the structure and properties of alpha-quartz. *Physics and*
171 *Chemistry of Minerals*, 46, 487-499.
- 172 Murri, M., Mazzucchelli, M.L., Campomenosi, N., Korsakov, A.V., Prencipe, M., Mihailova,
173 B.D., Scambelluri, M., Angel, R.J., and Alvaro, M. (2018) Raman elastic geobarometry
174 for anisotropic mineral inclusions. *American Mineralogist*, 103, 1869-1872.
- 175 Nestola, F., Alvaro, M., Casati, M.N., Wilhelm, H., Kleppe, A.K., Jephcoat, A.P., Domeneghetti,
176 M.C., and Harris, J.W. (2016) Source assemblage types for cratonic diamonds from X-
177 ray synchrotron diffraction. *Lithos*, 265, 334-338.
- 178 Nestola, F., Korolev, N., Kopylova, M., Rotiroti, N., Pearson, D.G., Pamato, M.G., Alvaro, M.,
179 Peruzzo, L., Gurney, J.J., Moore, A.E., and Davidson, J. (2018a) CaSiO₃ perovskite in
180 diamond indicates the recycling of oceanic crust into the lower mantle. *Nature*, 555, 237-
181 241.
- 182 Nestola, F., Nimis, P., Ziberna, L., Longo, M., Marzoli, A., Harris, J.W., Manghnani, M.H., and
183 Fedortchouk, Y. (2011) First crystal-structure determination of olivine in diamond:
184 Composition and implications for provenance in the Earth's mantle. *Earth and Planetary*
185 *Science Letters*, 305, 249-255.
- 186 Nestola, F., Prencipe, M., Nimis, P., Sgreva, N., Perritt, S.H., Chinn, I.L., and Zaffiro, G.
187 (2018b) Toward a Robust Elastic Geobarometry of Kyanite Inclusions in Eclogitic
188 Diamonds. *Journal of Geophysical Research: Solid Earth*, 123, 6411-6423.
- 189 Nimis, P., Alvaro, M., Nestola, F., Angel, R.J., Marquardt, K., Rustioni, G., Harris, J.W., and
190 Marone, F. (2016) First evidence of hydrous silicic fluid films around solid inclusions in
191 gem-quality diamonds. *Lithos*, 260, 384-389.
- 192 Nimis, P., Angel, R.J., Alvaro, M., Nestola, F., Harris, J.W., Casati, N., and Marone, F. (2019)
193 Crystallographic orientations of magnesiocromite inclusions in diamonds: what do they
194 tell us? *Contributions to Mineralogy and Petrology*, 174, Article n. 29.
- 195 Schmidt, C., and Ziemann, M.A. (2000) In-situ Raman spectroscopy of quartz: A pressure sensor
196 for hydrothermal diamond-anvil cell experiments at elevated temperatures. *American*
197 *Mineralogist*, 85, 1725-1734.
- 198 Tajcmanova L., Manzotti P., Alvaro M. (2020) Under pressure: High-pressure metamorphism in
199 the Alps, *Elements*, under review
- 200 Thomas, J.B., and Spear, F.S. (2018) Experimental study of quartz inclusions in garnet at
201 pressures up to 3.0 GPa: evaluating validity of the quartz-in-garnet inclusion elastic
202 thermobarometer. *Contributions to Mineralogy and Petrology*, 173, Article n. 42.
- 203 Zaffiro, G., Angel, R.J., and Alvaro, M. (2019) Constraints on the Equations of State of stiff
204 anisotropic minerals: rutile, and the implications for rutile elastic barometry.
205 *Mineralogical Magazine*, 83, 339-347.

206

207

208

209

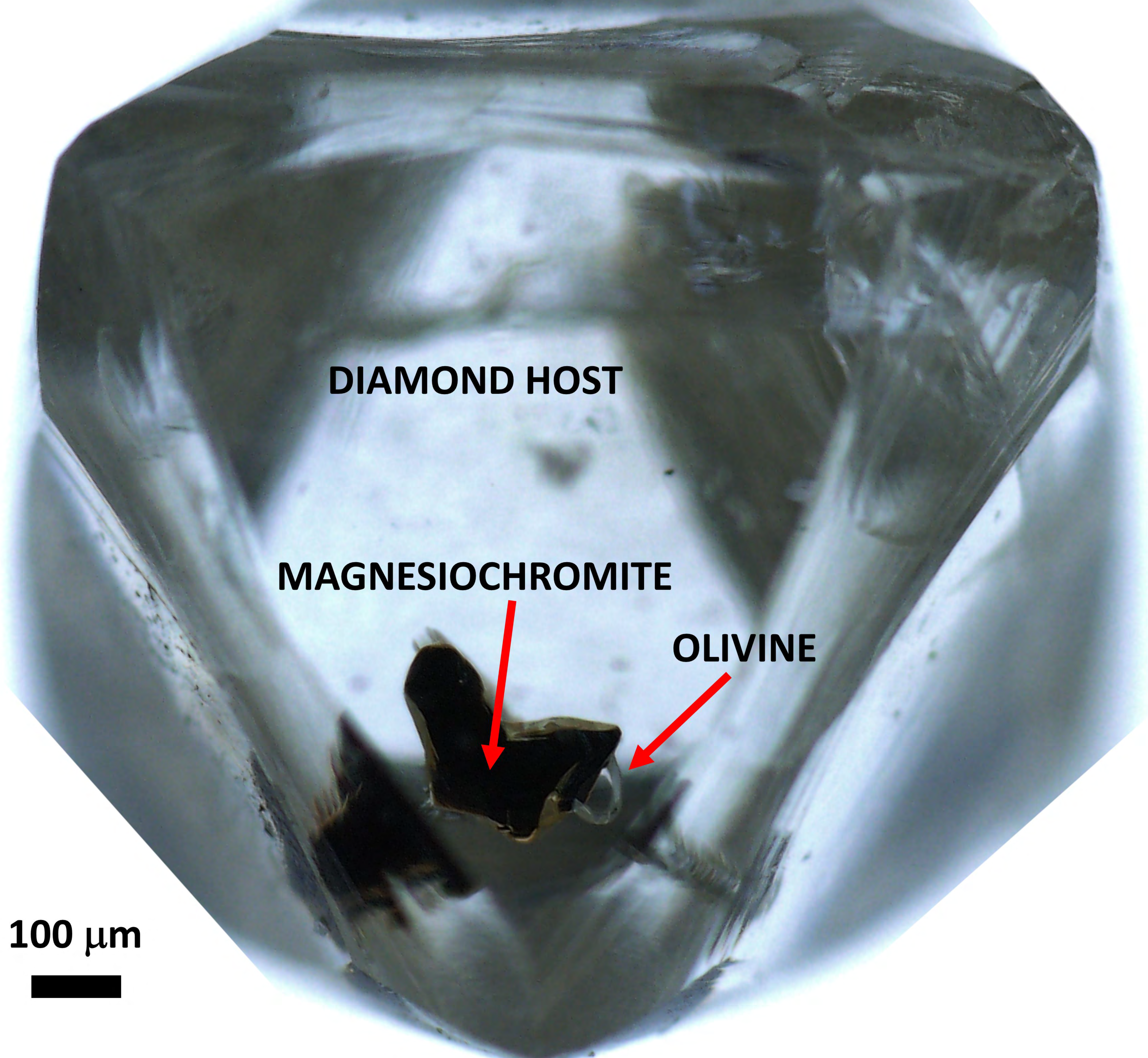
210 **Figure caption**

211

212 **Figure 1.** An example of a host-inclusion system. In this specific case, the transparent host is a
213 natural diamond from Udachnaya (Siberia, Russia), whereas the black inclusion is a
214 magnesiochromite spinel [$\sim(\text{Mg,Fe})(\text{Cr,Al})_2\text{O}_4$]. Magnesiochromite, in turn, has in contact a
215 second transparent inclusion, which is an olivine [$\sim(\text{Mg,Fe})_2\text{SiO}_4$] (the diamond was provided
216 by Dr. J.W. Harris, University of Glasgow; photo: Dr. Caterina Canovaro, University of Padova).

217

218



DIAMOND HOST

MAGNESIOCHROMITE

OLIVINE

100 μm

